研 究 速 報

Monolithically Integrated Diode Laser Detection System for Scanning Near-Field Optical Microscopy (SNOM): VCSEL Technology

Sabry KHALFALLAH*, Jean PODLECKI*, Masao NISHIOKA*, Christophe GORECKI**
Hideki KAWAKATSU**, Hiroyuki FUJITA*, Takao SOMEYA* and Yasuhiko ARAKAWA*

1. Introduction

When a Vertical Cavity Surface Emitting Laser (VCSEL) is submitted to a low level optical feedback both its output power and spectrum are modified according to the feedback. This effect known as self-mixing interference is the working principle of an optically active near-field detection system presented in this same issue[1].

In order for this near-field detection system to be practical and compact the main element i.e. the light source, namely the VCSEL, has to be electrically pumped. This article presents the results achieved so far in VCSEL technology.

2. Distributed Bragg reflectors

In typical VCSELs current is injected into the active region (containing quantum wells) through epitaxially grown reflector stacks known as distributed Bragg reflectors (DBR). These DBRs consist of several pairs of alternate quarter wavelength layers of different refractive indices, such as AlAs and GaAs. The DBRs are usually doped to form a p-i-n diode. The addition of dopants causes the Fermi level to lie close to the band edge in the doped regions and causes band bending to occur in the vicinity of the interfaces. The potential spikes thus existing at each interface result in a high resistance of the Bragg reflectors, especially p-doped reflectors[2].

*3 rd Department, Institute of Industrial Science, University of Tokyo
**2 nd Department, Institute of Industrial Science, University of Tokyo

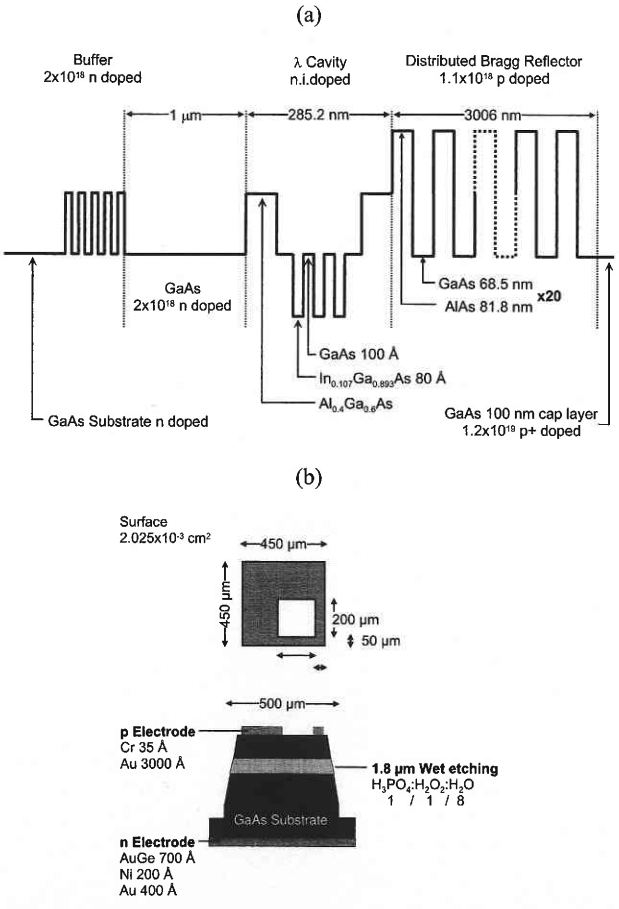

Fig. 1 (a) Band diagram of sample #1402 (b) Device structure of the LEDs fabricated from the MOCVD grown sample.

Fig. 1(a) presents the band diagram of a p-i-n light emitting diode (LED) whose active region consists of three strained InGaAs quantum wells (QWs), separated by GaAs barriers, and incorporated into a $Al_{0.4}Ga_{0.6}As$ λ cavity (λ= 950 nm). The n region consist of the substrate and buffer layers whereas the p region consists of 20 pairs of AlAs/GaAs quarter wavelength layers. This structure was grown by low pressure metal-organic chemical vapour deposition (LP-MOCVD) at 76 torr and 700°C; these standard growth conditions have been used throughout our study. From the grown sample we fabricated a 7×10 diode array by wet chemical etching of mesas using a H_3PO_4:H_2O_2:H_2O (1:1:8) solution. Joule evaporation was then used to deposit on top of the mesas Cr-Au p-type electrodes featuring a window and a backplane AuGe-Ni-Au n-type electrode. This process and the resulting device scheme, presented in Fig. 1, is common to all the devices we studied.

The current-voltage measurements performed on these diodes are presented in Fig. 2. The deduced resistance is found to have a mean value of 8 Ω. Since the I-V relation is non-linear, DBR resistance is very often expressed in terms of the voltage drop per pair at a typical injected current density of 1000 $A.cm^{-2}$. These diodes have a mean voltage drop of 0.875 V/pair which is comparable to published results.

The resistance of Bragg reflectors has to be reduced in order for the device to operate in continuous wave (CW) operation, otherwise the resulting heating is generally destructive and pulsed operation is required. We chose to reduce DBR resistance by inserting a 200 Å $Al_{0.5}Ga_{0.5}As$ layer between the GaAs and AlAs $\lambda/4$ layers. This results in the replacement of the single heterointerface with two junctions of smaller band offset, and thus carrier flow, both by tunnelling through and thermoionic emission over the resulting potential spikes, is made easier[3].

Fig. 3 presents the band diagram of sample #1414 which is similar to the previous one except for the 200 Å $Al_{0.5}Ga_{0.5}As$ layer inserted between the GaAs and AlAs $\lambda/4$ layers whose thicknesses have consequently been reduced. The Bragg reflector thus exhibits a staircase profile.

The current-voltage measurements performed on these diodes with staircase type reflector are presented in Fig. 4. The deduced resistance is found to have a mean value of 5.1 Ω which means a 36% reduction. When expressed in term of voltage drop per pair at the typical injected current density of 1000 $A.cm^{-2}$, the improvement is of 31% as these diodes present a mean voltage drop of 0.6 V/pair.

This improvement in the resistance of the Bragg reflectors is quite significant but might not allow CW operation of VCSELs. Further reduction would be achieved through the use of a special low oxygen aluminium source and the incorporation of modulation doped interfaces in which only the intermediate layers and the

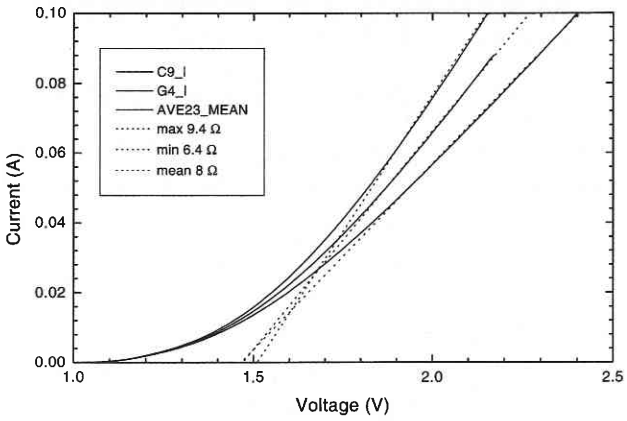

Fig. 2 I-V measurements on LEDs fabricated from sample #1402 (standard DBR).

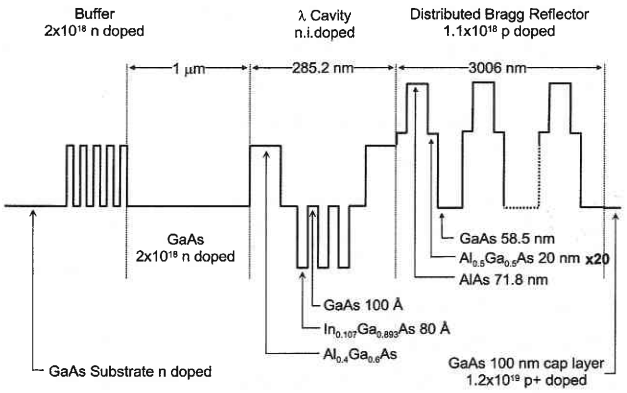

Fig. 3 Band diagram of sample #1414 (staircase DBR).

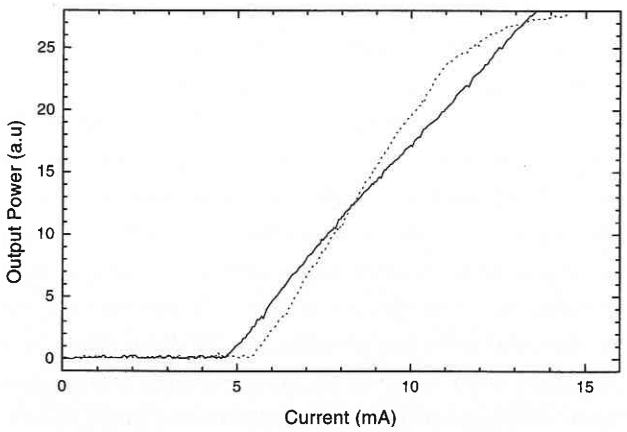

Fig. 4 I-V measurements on LEDs fabricated from sample #1414 (staircase DBR).

material immediately surrounding them are highly p-doped[4,5]. Voltage drops of few tens of mV/pair might then be obtained and CW operation achieved. Nevertheless VCSEL structure growth being not the main purpose of our MOCVD facility and optimal operation of the VCSEL being not the goal of our research project we decided to not further investigate this point.

3. Reflectivity and Photoluminescence spectra

Then we turned to the delicate problem of the precise matching of the reflectivity and emission spectra. Indeed since the operating wavelength is determined by the cavity and mirror dimensions, growth errors have effects on the cavity mode. An error of ±10% in the thickness of a 80 Å quantum well has a very small effect on the transition energies (~ ±3 nm) but an error of just ±1% in the thickness of the cavity will give a ±1% linear shift of the resonant wavelength i.e. ±10 nm for a nominal 1000 nm.

Fig. 6 presents the band diagram of a VCSEL structure whose active region consists of three InGaAs quantum wells (QWs), separated by GaAs barriers, and incorporated in the centre of a $Al_{0.4}Ga_{0.6}As$ λ cavity (λ = 950 nm), thus located at the antinode of the electromagnetic standing wave to be created in the device during operation. The bottom n-doped DBR consists of 33.5 pairs of $Al_{0.9}Ga_{0.1}As$/GaAs quarter wavelength layers with 200 Å $Al_{0.5}Ga_{0.5}As$ intermediate layers in order to reduce the resistance of the reflector. The top p-doped DBR consists of 20 pairs of $Al_{0.9}Ga_{0.1}As$/GaAs quarter wavelength layers incorporating $Al_{0.3}Ga_{0.7}As$ intermediate layers of 200 Å.

Note that the low index layers of the DBR consist of $Al_{0.9}Ga_{0.1}As$ instead of AlAs in order to ensure insensitivity to the aluminium oxidation process later used to partially transform the $Al_{0.98}Ga_{0.02}As$ layers immediately surrounding the cavity into AlxOy layers providing electrical insulation and current funnelling into the active region of the VCSEL structure.

Fig. 7 shows the reflectivity and photoluminescence spectra of this device. It can be seen that the reflectivity spectrum has the expected characteristics (position and width of the high reflectivity band) indicating that the DBRs are of good quality. The PL peak is at the expected wavelength but the cavity resonance and the PL peak are not matched since the QW PL peak is of the same order than the higher energy peak (due to the substrate) whereas the latter could not be noticed on Fig. 5(b). We deduced from these measurements that the cavity length required slight reduction and that its growth duration should be reduced from 139 s to 132 s.

We point out that, rather than fine optimisation of the growth conditions, the fabrication of a VCSEL array should allow us to obtain the expected results, that is to say pulsed laser operation at 950 nm.

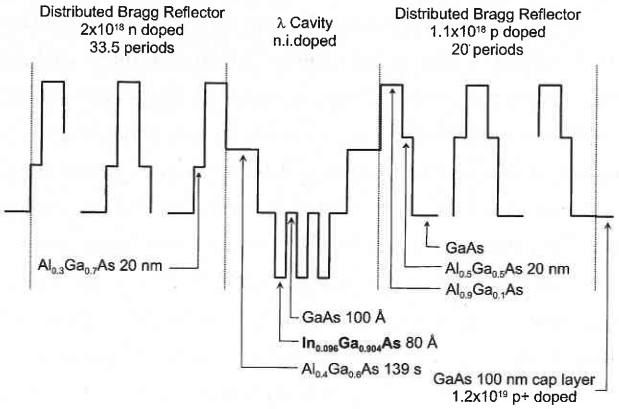

Fig. 5 Band diagram of sample #1544 (VCSEL).

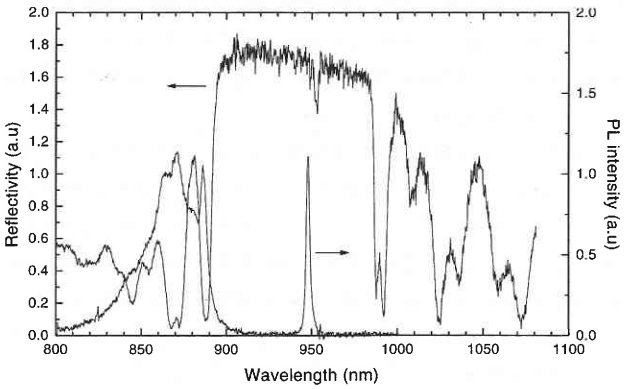

Fig. 6 Reflectivity and photoluminescence spectra of sample #1544.

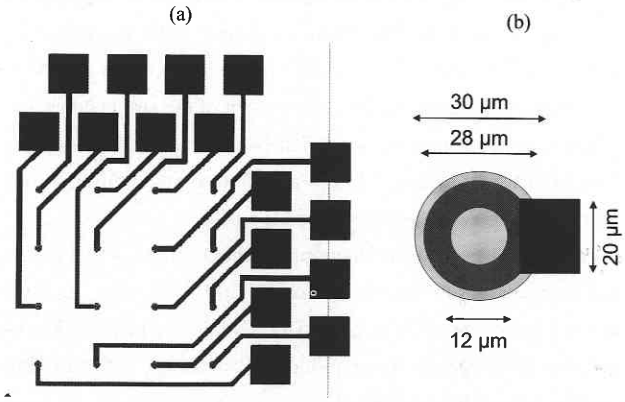

Fig. 7 (a) Scheme of a quarter of a the two-level photolithography mask of a 8 x8 VCSEL array (b) Schematic diagram of a mesa device featuring a top ring electrode connected to a routing wire.

4. VCSEL array

We have thus engaged in the design of an 8x8 individually

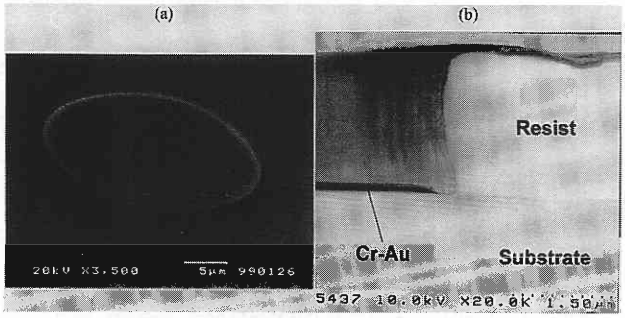

Fig. 8 Scanning electron micrographs of (a) a 2.5 μm high chemically etched mesa (b) a Cr-Au layer deposited by Joule evaporation through a reversed profile resist mask for further lift-off process.

addressed VCSEL array photolithography mask set consisting of two levels, the first one for mesa etching and the second one for metallization as can be seen in Fig. 8.

We first used these masks to study the delicate process steps to be used for the fabrication of the VCSEL array. The device geometry is defined by wet chemical etching. We used a H_3PO_4:H_2O_2:H_2O (1:1:8) solution and obtained quasi-vertical walls without excessive undercut as can be seen in Fig. 9(a) which shows the scanning electron micrograph of a 2.5μm high GaAs mesa. The mesas are then passivated through polyimide coating which also achieves quasi-planarisation of the array. After removal of the polyimide on top of the mesas, Cr-Au ring electrodes are deposited by Joule evaporation followed by a lift-off process. The latter is achieved through the use of a reversed profile resist (cf. Fig. 9(b)) which allows easy removal of the resist and excess metal by rinsing in acetone.

5. Conclusion

The results of the investigation of VCSEL technology should lead to the fabrication of a VCSEL array, operating at 950 nm in pulsed operation, in the near future. The further use of Reactive Ion Etching instead of wet chemical etching should also result in an improvement of the device features. Future work will consist in the integration of a photodetector and a sharp tip with the VCSEL. This should result in a breakthrough in scanning near-field optical microscopy.

Acknowledgements

The authors would like to express their thanks to the Japanese Society for the Promotion of Science (JSPS) and the Ministry of Education, Science, Sports and Culture (Monbusho) for their financial support.

(Manuscript received, June 28, 1999)

References

1) S. Khalfallah, et al, "Monolthically Integrated Diode Laser Detection System for Scanning Near-Field Optical Mictoscopy (SNOM) : Study of the Optical Feedback Effect in VCSELs", this same issue.
2) T.E. Sale, "Vertical Cavity Surface Emitting Lasers", Research Studies Press, 1995.
3) K. Tai, L. Yang, Y.H. Wang, J.D. Wynn and A.Y. Cho, "Drastic reduction of series resistance in doped semiconductor distributed Bragg reflectors for surface-emitting lasers", Appl. Phys. Lett., vol.56, no. 25, pp. 2496-2498, 1990.
4) K. Kojima, et al., "Reduction of p-doped mirror electrical resistance of GaAs/GaAlAs vertical-cavity surface-emitting lasers by delta doping", Electron. Lett., vol. 29, no. 20, pp.1771-1772, 1993.
5) M.G. Peters, et al., "Band-gap engineered digital alloy interfaces for lower resistance vertical-cavity surface-emitting lasers", Appl. Phys. Lett., vol. 63, no. 25, pp. 3411-3413, 1993.